TELKOMNIKA Indonesian Journal of Electrical Engineering
Vol.12, No.4, April 2014, pp. 2516 ~ 2529
DOI: http://dx.doi.org/10.11591/telkomnika.v12i4.4443

Influence of Non-Integer Harmonics and Interference on SAPF

Zhang Chao*[1,b], Ren Zi-Hui[1], Zhang Yi-Jun[2,b], Ma Xiao-Ping[1]
[1]School of Information and Electrical Engineering, CUMT
[2]Longkou Mineral Group Co. Ltd, 265700 Longkou, China
Corresponding author, e-mail: diy007_z@163.com[a], lunwenzzz@163.com[b]

Abstract
Inter-harmonics and non-periodic disturbance generated by aging SAPF or other reasons would impact SAPF performance. In this paper, three-level SAPF was used as example: the mathematical model of three-level SAPF under the definition of virtual flux was built. The power theory under the definition of CPT was discussed. Based on the definition of CPT, the method for SAPF detection system with CPT was studied and the performance was verified by comparing results with the PQ theory. Repetitive control and PI control were used as a combination system for grid inter-harmonics compensation. EID controller was used to improve the performance of repetitive controller for inter-harmonics and non-periodic disturbance rejection. Finally, system reliability was verified by MATLAB simulation and three-level experiment platform.

***Keywords**: inter-harmonic, conservative power theory (CPT), equivalent input-disturbance (EID), repetitive control*

1. Introduction

Inter-harmonic means that harmonic components which frequency is not equal to the fundamental and multiple fundamental frequency [1]. With the application of HVDC equipment, electric arc furnaces, converters and other power electronic equipments, inter-harmonics were produced [2, 3]. Inter-harmonics have similar hazards with harmonics. More seriously, they also can cause voltage flicker and impact torque [4]. As frequencies of inter-harmonics have always been changed with different operating conditions of harmonic source equipments, inter-harmonics is difficult to be accurately detected and eliminated.

SAPF has been widely used to resolve harmonic pollution issues. For the design of SAPF, different grid environments and load requirements should be considered. SAPF should be able to run at different complex grid environments, and do not make interference to the grid. At present, the research focuses of inter-harmonic are on the detection method. The harmonic suppression method, is mainly used with passive filters. The way that using SAPF to eliminate inter-harmonic content was less studied. And existing harmonic detection and control methods of SAPF are not effective for inter-harmonics environment [5]. So, it is significant to do the research for the inter-harmonics and harmonics detection and compensation methods based on SAPF.

Currently, detection methods of harmonics and inter- harmonics can be divided into two categories: frequency-domain and time-domain. Harmonic current can be obtained by frequency-domain detection methods [6-9]. But these methods are characterized by large amount of calculation, and poor real-time performance. The existing time-domain detection methods are based on non-sinusoidal power theory, and they are applicable for SAPF. These methods are simple in structure, and they are widely used. There are two types of commonly used time-domain detection methods which based on the power theory, the instantaneous power theory and the Fryze power theory. The harmonic current can not be accurately detected by method with traditional instantaneous reactive power theory (p-q theory) when three-phase voltage is unbalance and waveform is distorted [10]. Harmonic and reactive current detection problems can be solved by universal instantaneous power theory and its improved algorithm when the three-phase voltage is unbalance and waveform is distorted [11, 12]. FBD method was proposed by Fryze, and improved by Buchholz and Dpenbrock. By separating the current

Received August 17, 2013; Revised October 31, 2013; Accepted November 15, 2013

with concept of equivalent conductance, the physical meaning of the current component was discussed. And compared to the traditional instantaneous power definition, without coordinate transformation, FBD method was characterized by a relatively simple algorithm [13, 14]. The instantaneous power was defined by CPT (conservative power theory) in the three phase unbalance and distortion system [15]. Compared to the p-q power theory and FBD power theory, the unbalanced and distortion current is more accurately expressed by CPT theory [16, 17]. But it needs further study for the grid with inter-harmonics situation.

The periodic reference signal or the periodic interference signal will be controlled by repetitive control method. And when it combined with PI control, or predictive control, the PWM converter can get better control performance for current. But repetitive control performance for non-periodic signal, or non-periodic interference signal is poor. Therefore, it is important to improve the control system for better non-periodic control performance. There are two ways to improve the performance, HORC (high-order repetitive controller) [18, 19] and adaptive repetitive controller [20]. Though the control performance can be improved by these methods, the complexity of the system will be increased, and it will be difficult to achieve system stability. If we consider the non-periodic signals as interference, the disturbance observer can be used to improve the non-periodic control performance of repetitive controller. EID (equivalent input disturbance) observer [21] is different with the usual disturbance observer, which is not based on the inverse system theory, but based on an active disturbance rejection method. This method is simple to implement and can be used for repeatedly controller to improve the non-periodic disturbance rejection performance.

In this paper, the model of three-level SAPF was built. SAPF directive harmonic current detection method under the inter-harmonic environment based on the definition of CPT power theory was studied. Both the repetitive control and PI control was used for the grid current harmonics and inter-harmonics compensation. By introducing EID controller improves the SAPF control performance for non-periodic signal interference. Analysis of the designed system stability and sensitivity of the issue. Gives a suitable inter-harmonics environment SAPF system design methodology. Simulation and experiment show that the designed system can accurately detect harmonic, inter-harmonic content, effective on the grid to compensate harmonics and inter-harmonics.

2. Mathematic Model of Three-level SAPF on Virtual Flux Oriented

The main circuit topology of SAPF is a diode-clamped three-level inverter. Three kinds of switch state can be obtained by four switches of each phase leg from three-level converter, which is shown in Figure 1(a). According to the concept of the flux in motor speed control, by spatial coordinate transformation, vector diagram of the virtual-flux oriented system can be drawn as shown in Figure 1(b).

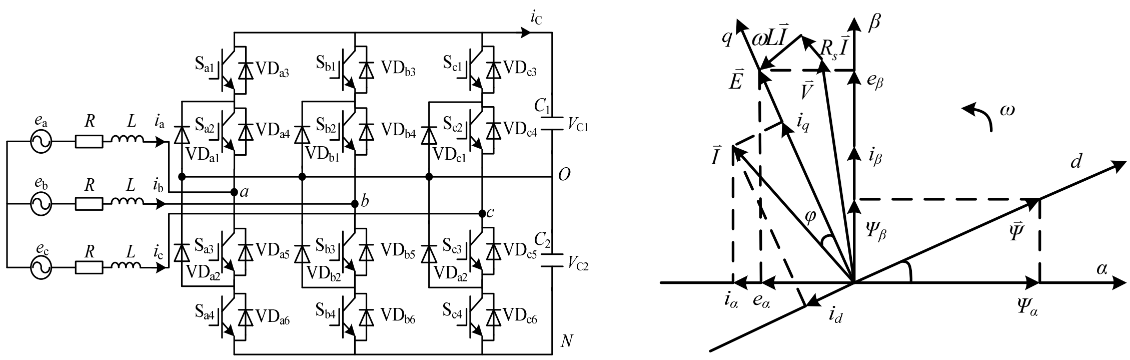

(a) The topology of three-level converter

(b) Vector diagram of the virtual-flux oriented system

Figure 1. Three-level SAPF on Virtual Flux Oriented

According to Kirchhoff law and the structure shown in Figure 1, state-space expression of SAPF in dq reference frame is given directly by:

$$Z\dot{X} = AX + Be$$

Where, $Z = diag[L \quad L \quad C_1 \quad C_2]$, $X = [i_d \quad i_q \quad V_{C1} \quad V_{C2}]^{\mathrm{T}}$, $B = diag[1 \quad 1 \quad 0 \quad 0]$, $e = [0 \quad \sqrt{\frac{3}{2}}V_m \quad 0 \quad 0]^{\mathrm{T}}$

$$A = \begin{bmatrix} -R & \omega L & -S_{d1} & S_{d2} \\ -\omega L & -R & -S_{q1} & S_{q2} \\ S_{d1} & S_{q1} & 0 & 0 \\ -S_{d2} & -S_{q2} & 0 & 0 \end{bmatrix}$$

3. The Inter-harmonic Detection Method Based on CPT Theory

3.1. The CPT Framework

CPT theory, which has been put forward in recent years, is power definition method under the nonlinear time-domain condition. For a continuous variable x(t), over period T, the original function and derivative function can be defined as follows:

$$x'(t) = \int_0^t x(\tau)\mathrm{d}\tau \; ; \; x''(t) = \frac{\mathrm{d}}{\mathrm{d}t}x(t)$$

The DC component is defined as:

$$\bar{x}' = \frac{1}{T}\int_0^T x'(t)\mathrm{d}t$$

Considering ω=2π/T, homo-variable of x can be defined as:

$$\hat{x} = \omega(x' - \bar{x}') \; ; \; \breve{x} = \frac{1}{\omega}x''$$

Note that $\hat{x}$ and $\breve{x}$ are dimensionally homogeneous to x, and they are equal in the amplitude of the resultant signals, so we called *x*, $\hat{x}$ and $\breve{x}$ the homo-variables. According to the definition of CPT theory, for three-phase system,

Active power P is defined as:

$$P = \langle \boldsymbol{u}, \boldsymbol{i} \rangle = \frac{1}{T}\int_0^T u(t) \cdot i(t)\mathrm{d}t$$

Reactive power Q is defined as:

$$Q = \langle \hat{\boldsymbol{u}}, \boldsymbol{i} \rangle = \frac{1}{T}\int_0^T \hat{u}(t) \cdot i(t)\mathrm{d}t$$

Active current ia is defined as:

$$i_a = \frac{P}{\|u\|^2}u = G_a \cdot u \tag{1}$$

Reactive current ir is defined as:

$$i_r = \frac{Q}{\|\hat{u}\|^2}\hat{u} = B_r \cdot \hat{u} \tag{2}$$

Void current iv is defined as:

$$i_v = i - i_a - i_r$$

3.2. The Inter-harmonic Detection Method Based on CPT Theory

In order to use the CPT theory to detect SAPF three-phase harmonic current, assuming three-phase sinusoidal and balance system, with the initial phase of supply voltage which equals to 0, per unit voltage can be expressed as:

$$\begin{cases} e_a = \sin(\omega t) \\ e_b = \sin(\omega t - \frac{2\pi}{3}) \\ e_c = \sin(\omega t + \frac{2\pi}{3}) \end{cases}$$

Where, e_a, e_b and e_c are three phase per unit supply voltage, and ω is the angular frequency. According to CPT definition, homo-variable of ea can be expressed as:

$$\begin{cases} \hat{e}_a = -\cos(\omega t) \\ \breve{e}_a = \cos(\omega t) \end{cases}$$

The three-phase load current is given by:

$$\begin{cases} i_a = \sum_{h=1}^{\infty}[I_h^+ \sin(h\omega t - \theta_h^+) + I_h^- \sin(h\omega t - \theta_h^-) + I_h^0 \sin(h\omega t - \theta_h^0) \\ i_b = \sum_{h=1}^{\infty}[I_h^+ \sin(h\omega t - \frac{2\pi}{3} - \theta_h^+) + I_h^- \sin(h\omega t + \frac{2\pi}{3} - \theta_h^-) + I_h^0 \sin(h\omega t - \theta_h^0) \\ i_c = \sum_{h=1}^{\infty}[I_h^+ \sin(h\omega t + \frac{2\pi}{3} - \theta_h^+) + I_h^- \sin(h\omega t - \frac{2\pi}{3} - \theta_h^-) + I_h^0 \sin(h\omega t - \theta_h^0) \end{cases}$$

Where, ia, ib and ic are the three-phase load current. I is the amplitude of the harmonic current. θ is the initial phase angle of the harmonic current. Subscript h is the harmonic number. When h = 1, it indicates the fundamental component; when h is integer, it means multiple fundamental frequency components; when h is non-integer, it indicates the harmonic components. Superscript +, - and 0 represent positive, negative and zero sequence component.

According to CPT definition, taking into the voltage and current expressions, it can be calculated as:

$$P = \frac{3}{2}\{I_1^+ \cos\theta_1^+ + I_1^- \cos(2\omega t - \theta_1^-) + \sum_{h=2}^{\infty}[I_h^+ \cos((h-1)\omega t - \theta_h^+) + I_h^- \cos((h+1)\omega t - \theta_h^-)]\} \tag{3}$$

If AC component of equation (1) was filtered off, linear active power can be obtained as:

$$\overline{P} = \frac{3}{2} I_1^+ \cos\theta_1^+ \tag{4}$$

Note that Equation (4) corresponds with the fundamental current active component.

According to CPT theory, homo-variables of three-phase supply voltage can be defined as:

$$\begin{cases} \hat{e}_a = -\cos(\omega t) \\ \hat{e}_b = -\cos(\omega t - \frac{2\pi}{3}) \\ \hat{e}_c = -\cos(\omega t + \frac{2\pi}{3}) \end{cases}$$

According to the reactive power definition of CPT theory, instantaneous reactive power Q can be obtained as:

$$Q = \frac{3}{2}\{-I_1^+ \sin\theta_1^+ + I_1^- \sin(2\omega t - \theta_1^-) + \sum_{h=2}^{\infty}[I_h^+ \sin((h-1)\omega t - \theta_h^+) + I_h^- \sin((h+1)\omega t - \theta_h^-)]\} \quad (5)$$

If AC component of Equation (3) was filtered off, linear reactive power can be obtained as:

$$\overline{Q} = -\frac{3}{2} I_1^+ \sin\theta_1^+ \quad (6)$$

Taking the Equation (4) and Equation (6) into Equation (1) and Equation (2), the fundamental positive sequence component can be got by the addition of the two final equations. Besides the fundamental positive sequence component, the rest components is the SAPF harmonic detection signal. Based on CPT power definition, SAPF harmonic detection system is shown in Figure 2.

Considering ip-iq detecting method based on instantaneous reactive power theory as a comparison, the grid inter-harmonic detection effect of the system, which was shown in Figure 2, can be verified by simulation. The fundamental frequency of testing wave was 50Hz. The harmonic components which frequencies were 80Hz and 250Hz, were added at Time=0.08s. The simulation results were shown in Figure 3.

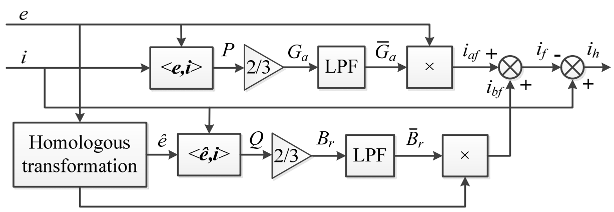

Figure 2. Harmonic Detection System Based on CPT

The waveform ia and the fundamental detection waveforms which detected by ip-iq method and CPT method, were shown in the Figure 3(a). Note that, before adding the harmonic component, the fundamental detection waveform got by CPT method can coincide with ia. But for the waveform got by ip-iq method, there is a certain phase offset, which is caused by the coordinate transformation of the instantaneous power theory. Subtracted the fundamental detection waveform and ia, the harmonic component can be obtained, which was shown in Figure 3(b). It can be shown as that, since there is phase offset phenomenon, the amplitude of harmonic component detected by ip-iq method was finally amplified.

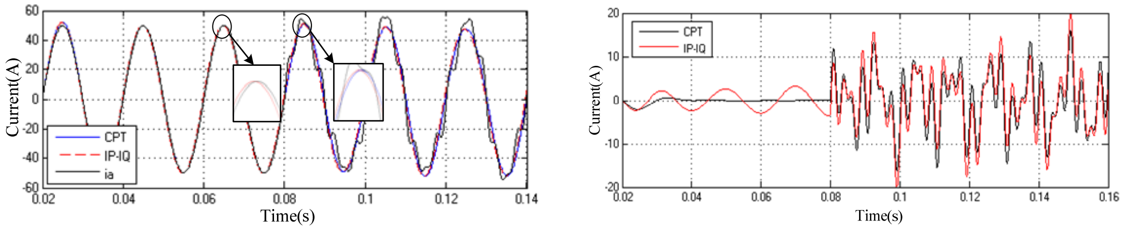

(a) Fundamental detection waveform (b) Harmonic detection waveform

Figure 3. Comparison of Current Waveforms

4. Compensation System Based on EID and Repetitive Controller

4.1. Sensitivity Analysis of Control System

Sensitivity is an important indicator of system performance. For the control system shown in Figure 5(a), sensitivity is defined as the transfer function from the external disturbance d to the output y of plant. It can also be defined as the function from the external input signal r to the error signal e. Therefore, the sensitivity reflects the tracking performance of the input signal and the disturbance suppression performance. The sensitivity function *S* of the control system shown in Figure 5(a), is given by:

$$S=\frac{E(z)P(z)}{R(z)}=\frac{Y(z)}{D(z)}=\frac{P(z)}{1+\left[H(z)+G_R(z)\right]P(z)} \tag{7}$$

In addition to consider the mathematical model and performance indicators, the design of control system should also be subject to certain constraints. Sensitivity function is the important performance indicator of the control system. But it can not be any value. It should to be bound by the Bode integral theorem. According to Bode integral theorem, the sensitivity integral is a constant. If the control system is stable, the integral will be zero, which means:

$$\int_0^\infty \ln\left|S(\mathrm{j}\omega)\right|\mathrm{d}\omega=0 \tag{8}$$

When S<1, the logarithmic sensitivity is negative; when S> 1, the logarithmic sensitivity is positive. Therefore, according to Equation (8), it is required that the sensitivity integral will be zero, the area when the logarithmic sensitivity is positive equals to the area of negative logarithmic sensitivity. Although the smaller sensitivity can be got, it will be better performance of the control system. According to Bode integral theorem, if the sensitivity is reduced in a certain frequency band, it will be rose in the other bands. Sensitivity will be reduced in the periodic signal band by repetitive control, but it will be increased in non-periodic bands, resulting in performance deterioration of non-periodic signal control.

For repetitive control system, sensitivity function S_r is given by:

$$S_r=\frac{Y(z)}{D(z)}=\frac{P(z)}{1+G_{RE}(z)P(z)} \tag{9}$$

Where, $G_{RE}=\dfrac{k_r z^k S(z)}{z^N-Q(z)}$

For repetitive and PI control system, sensitivity function S_p is given by:

$$S_p=\frac{P(z)}{1+\left[G_{RE}(z)+G_{PI}(z)\right]P(z)} \tag{10}$$

Where, $G_{PI}(z) = K_P z^{-1} + \frac{K_I}{z-1}$

For the control system shown in Figure 5(c), sensitivity function S_e is given by:

$$S_e = \frac{P(z)}{1 + [G_{RE}(z) + G_{PI}(z) + H(z)]P(z)} \quad (11)$$

Where, $H(z) = B^+ L \frac{F(z)}{1-F(z)}[G_R(z)G_1(z) + \frac{1}{1+G_2(z)}]$

$G_R(z) = G_{RE}(z) + G_{PI}(z)$, $G_1(z) = C[zI - (A - LC)]^{-1}B$, $G_2(z) = C[zI - A]^{-1}L$

From Equation (9) to Equation (11), it can be seen that, after the addition of PI controller and EID controller, by adjusting the transfer function value of the PI and EID controller, the system sensitivity function value can be decreased.

According to equations from Equation (9) to Equation (11), it is shown in Figure 4 that sensitivity function comparison among the repetitive control system, the repetitive and PI control system, and the control system adding with EID controller. It can be seen that the sensitivity function value of repetitive controller is low at the fundamental frequency 50Hz and its multiple frequencies. While at the non-periodic position between the fundamental multiple frequencies, sensitivity function value is at a high point. Therefore, the repetitive controller has a good tracking or inhibition performance for the fundamental and multiple frequencies signal. And for inter-harmonics and non-periodic disturbance to SAPF, the control performance is deteriorated.

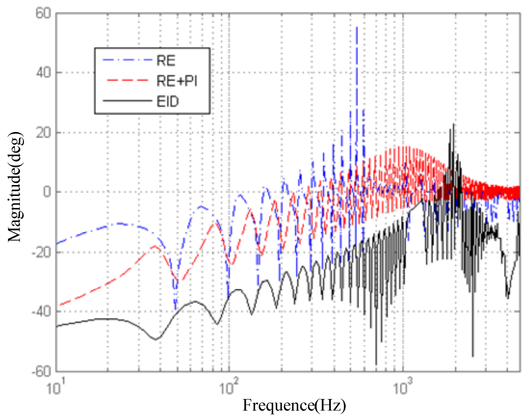

Figure 4. The Sensitivity Comparison of Control System

From Figuree 4 it can be seen, adding with PI and EID controller, the sensitivity function value is decreased overall low frequencies band. It means that system control performance gets better for the fundamental and multiple frequencies signal and the non-periodic interference signal, in accord with the control law embodied in Equation (7). Meanwhile, according to the Bode integral theorem and as it has shown in Figure 4, introduction of EID controller make a control performance deterioration during some high frequencies. The main function of SAPF is to compensate the grid characteristic harmonic content with low frequencies. Although the introduction of EID controller makes the deterioration of system control performance for some high-frequency signal, but it will not impact practical application performance of SAPF.

4.2. Design of Control System

According to the three-level SAPF model, based on the EID and repetitive control method, SAPF current compensation control system was designed, as shown in Figure 5(a).

The SAPF compensation signal, which is the harmonic current components besides the fundamental current component, mainly contains multiple fundamental frequency components. When the content of the grid inter-harmonics are obvious, it means the compensation signal is mixed with non-integer multiple fundamental frequency signal. These non-periodic signals can not be controlled by repetitive controller.

Complex repetitive control system consists of improved repetitive controller and PI controller, which are connected in parallel. The periodic signal can be controlled by repetitive controller, so the SAPF compensation accuracy will be improved. And non-periodic signal can be controlled by PI controller, which can also adjust the delay time by repetitive controller, so the dynamic performance of SAPF will be improved. The control system is shown in Figure 5(b).

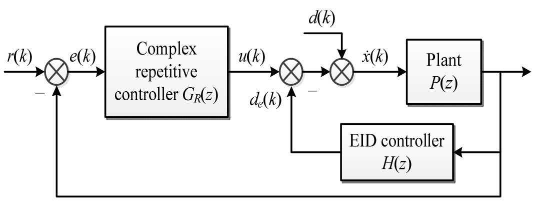

(a) SAPF current compensation control system

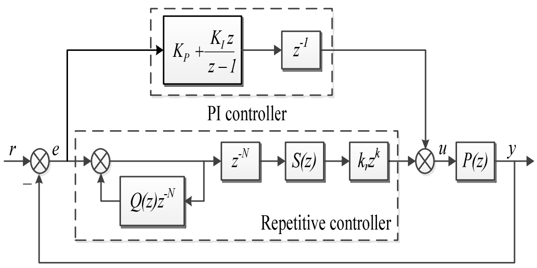

(b) Complex repetitive control system

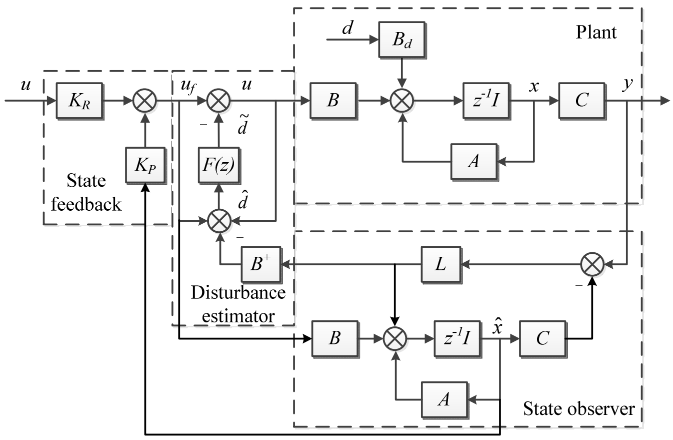

(c) EID control system

Figure 5. The Current Compensation System of SAPF

With the aging of APF devices, devices parameters will be volatile. Furthermore, with dead band plus effect, the load fluctuation and other factors, the periodic and non-periodic disturbances will appear in the actual operation of SAPF. For the repetitive controller, the periodic interference can be eliminated. But the effect of non-periodic disturbance control will deteriorate. This paper introduces the equivalent input disturbance method for non-periodic signal interference suppression, so the robustness of SAPF current compensation controller and the SAPF compensation effect can be improved.

4.3. Stability Analysis of Control System

System stability design is the most basic requirement for control system. Only based on the stable control system, the further system design, considering the rest of the system performance requirements, could be continued.

As it is shown in Figure 5(a), the control system can be seen as two subsystems which are the complex repetitive PI control system and the EID control system in series. The stability of the control system, could be considered as two subsystems both are stable. As control parameters of the composite repetitive control system and the EID control system are without overlap, the two subsystems can be designed individually. For the composite repetitive control system, which is shown in Figure 5(b), considering the transfer function of the PI controller $G_{PI}(z)$, the characteristic equation is given by:

$$\Delta = [1+G_{PI}(z)P(z)]\left[z^N - Q(z) + \frac{k_r z^k S(z)P(z)}{1+G_{PI}(z)P(z)}\right]$$

There are two parts in the characteristic equation of complex repetitive control system. It is easy to see that the characteristic equation is $1+G_{PI}(z)P(z)$, when the system is controlled by PI controller individually. The latter part is the characteristic equation when the repetitive controller add to the system. Therefore, the stability of complex repetitive control system required, based on the stable separate PI control system, the complex control system is also stable after the addition of repetitive controller.

In order to analyze the stability of the control system, by setting input signal and interference signal of the system shown in Figure 5(a) to zero, taking the input and output of low-pass filter F(z) in the interference estimator as the system input and output, the EID control system shown in Figure 5(c) is equivalent to the system shown in Figure 6. The component in the dotted-line G(z) is given by:

$$\begin{aligned} G(z) &= 1 - B^+ LC[zI-(A-LC)]^{-1}B \\ &= B^+(sI-A)[zI-(A-LC)]^{-1}B \end{aligned}$$

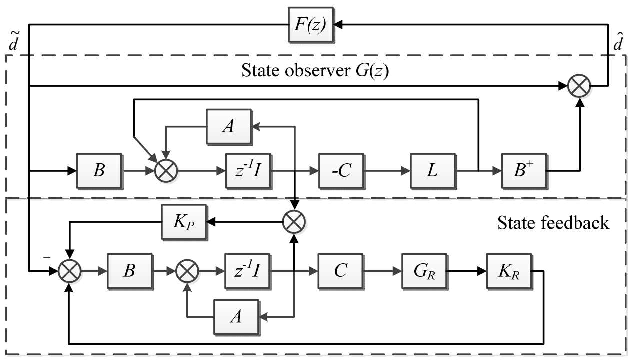

Figure 6. The Equivalent Control System of EID

As it is shown in Figure 6, EID system is divided into three parts, the state observer, the low-pass filter and the state feedback section. As state feedback section will not affect other system stability, it can be designed as independent part according to the LMI or optimal control method. According to the small gain theory, under the premise that state observer and low-pass filter are stable, it is need to meet that the H_∞ norm of system transfer function is less than 1 for the entire system stability, which means:

$$\|F(z)G(z)\|_\infty < 1 \qquad (12)$$

4.4. Design of Control System

Therefore, the design of observer gain *L* can be converted into a standard output feedback H_∞ problem. The new input ω(t) and the new output *z*(t) were set for the low pass filter *F*(s). So the state space expression can be given:

$$\begin{cases} \dot{\hat{x}}(t) = A\hat{x}(t) + B\tilde{d}(t) - u(t) \\ z(t) = d(t) - B^{+}u(t) \\ y(t) = C\hat{x}(t) \end{cases}$$

$$\begin{cases} \dot{x}(t) = Ax(t) + B\omega(t) \\ \tilde{d}(t) = Cx(t) \end{cases}$$

For the system was shown in Figure 6. The G and F system can be given as:

$$GF = \left\{ \begin{bmatrix} A & 0 \\ BC & A \end{bmatrix}, \begin{bmatrix} B & 0 \\ 0 & -I \end{bmatrix}, \begin{bmatrix} C & 0 \\ 0 & C \end{bmatrix}, \begin{bmatrix} 0 & -B^{+} \\ 0 & 0 \end{bmatrix} \right\}$$

It is need to design output feedback controller ***u=Ly*** to make equation (7) holds. So we can get *L* to satisfy that:

$$\lim_{\delta \to \infty} \left[sI - (A - LC) \right]^{-1} B = 0$$

According to the discussion above, the steps of design can be given as follows:
Step 1: Design system feedback gain K_p, K_r;
Step 2: The low pass filter F(s) should be designed to make equation as follows holds;

$$\begin{cases} |F(j\omega)| \approx 1, & \omega \le \omega_{\max} \\ |F(j\omega)| < 1, & \omega > \omega_{\max} \end{cases}$$

Where, ω_{max} is maximum angular frequency of non-periodic disturbance.
Step 3: Design the observer gain *L*, to make the G(s) stable;
Step 4: Adjust the parameters until the system meets the requirements.
These design steps are very intuitive and easy to understand. The adjustment process of the design is very simple.

5. Simulation and Experimental Verification

In order to verify the designed SAPF control performance, based on the Matlab software and three-level experiment platform, simulation and experimental model of SAPF control system was established, which was shown in Figure 7.

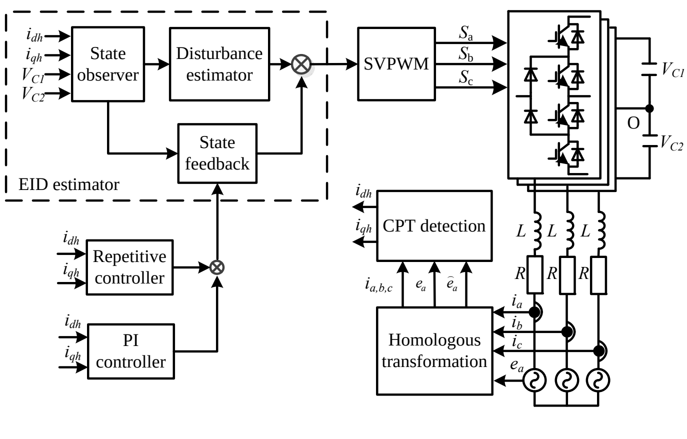

Figure 7. Three-level SAPF control system structure.

Three-phase grid current, voltage and their homologous variables were detected by three-level SAPF. Without coordinate transformation, harmonic current detected by the CPT method was taken into the controller. After the interference suppression by EID controller, the switch control signal was got by the three-level SVPWM modulation, which was used to make the three-level SAPF generate compensation current, which can offset harmonic component of grid current. Harmonic source in Figure 7 was three-phase uncontrolled rectifier with resistive load.

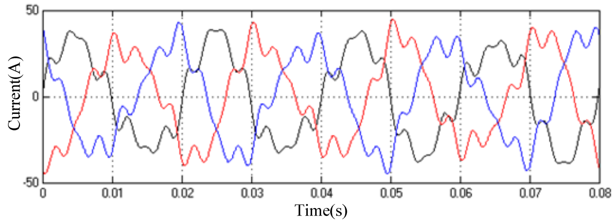

(a) Current waveform before compensation

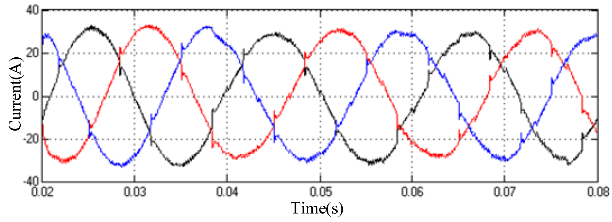

(b) Current waveform after compensation

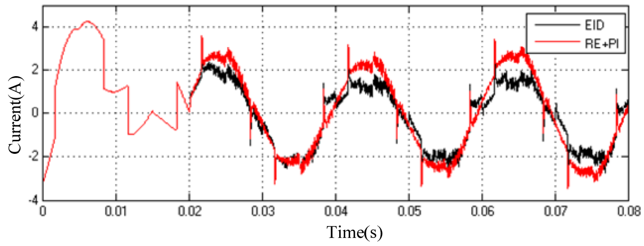

(c) Error between compensation current and reference current

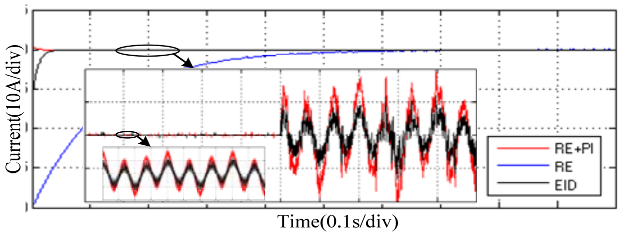

(d) Error between compensation current and reference current.

Figure 8. Comparison of SAPF Harmonic Compensation.

Simulation system built by Matlab was shown in Figure 7. Grid current waveform before the compensation was got in Figure 8 (a). After the compensation by SAPF, the grid current waveform was got in Figure 8 (b). Make the simulation for the two systems with and without the EID controller. Subtracted the compensation current from the detected harmonic current command to obtain the error current signal as it was shown in Figure 8 (c). As it can be seen, the error between compensation current and reference current has been smaller by addition of EID controller. It indicates that by adding EID controller, the better tracking performance can be got for the control system.

It was error curve shown in Figure 9 (d) between the compensation current and the reference current, of the system with non-periodic disturbance *d*. After the addition of d=10sin(180πt) at t=0.2s to the system, of which fundamental frequency was 50Hz, we can see that whether the system is with non-periodic disturbance or not, the error of the system with EID controller, between the compensation current and the reference current is less than it in the repetitive and PI control system.

Based on the three-level experiment platform, by detection on the grid current with Fluke power quality analyzer, waveform and spectrum can be obtained as they were shown in Figure 9. The experimental parameters were shown in Table 1. Before the compensation by SAPF, the characteristic harmonics of source was 5th and 7th harmonics, and there was also 1.5th inter-harmonic in the grid. Waveform and spectrum of grid current were shown in Figure 9 (a) and (b). SAPF with the repetitive and PI controller was used to compensate harmonics and inter-harmonics in the grid. Current waveform and spectrum were shown in Figure 9 (c) and (d). With the control system shown in Figure 7, waveform and spectrum of system current after compensation were obtained, shown in Figure 9 (e) and (f). As it can be seen, by the comparison between the system designed in this paper and the repetitive and PI control system, the effect of harmonic compensation is more obvious with the new system.

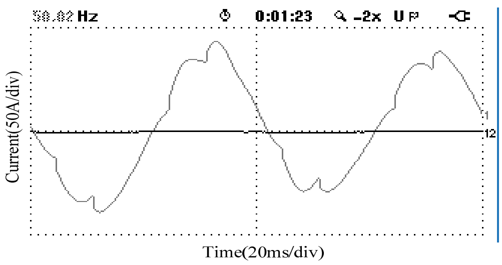

(a) Current waveform before compensation

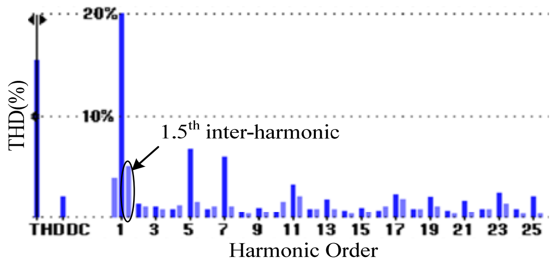

(b) Current waveform after compensation

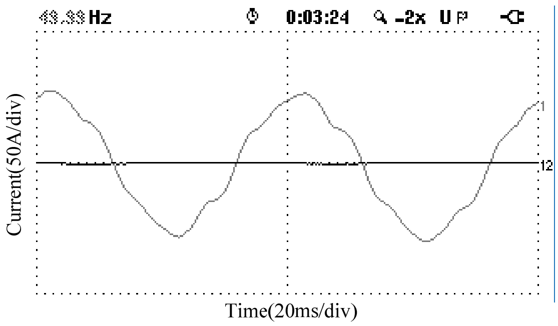

(c) Current waveform by repetitive and PI control

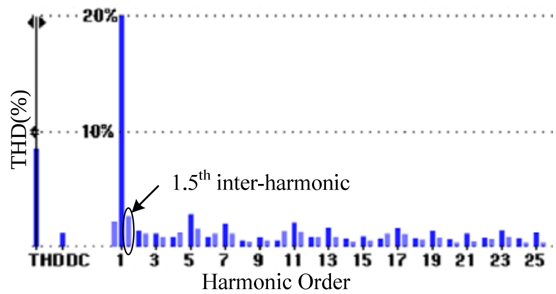

(d) Current spectrum by repetitive and PI control

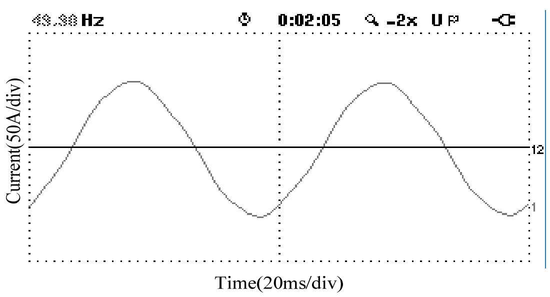

(e) Current waveform by EID control

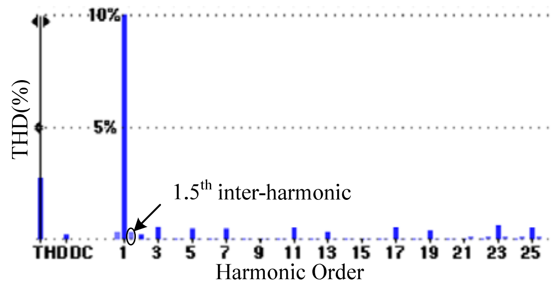

(f) Current spectrum by EID control

Figure 9. Comparison of Compensation Effects For Grid Current.

6. Conclusion

In this paper, the model of three-level SAPF was built. SAPF directive harmonic current detection method under the inter-harmonic environment based on the definition of CPT power theory was studied. Both the repetitive control and PI control was used for the grid current harmonics and inter-harmonics compensation. By introducing EID controller improves the SAPF control performance for non-periodic signal interference. Analysis of the designed system stability and sensitivity of the issue. Gives a suitable inter-harmonics environment SAPF system design methodology. Simulation and experiment show that the designed system can accurately detect harmonic, inter-harmonic content, effective on the grid to compensate harmonics and inter-harmonics.

Acknowledgment

The authors would like to thank China National Natural Science Foundation (51077124) and Graduate Student Research and Innovation Program of Jiangsu Province (CXZZ13_0931)

References

[1] IEEE Standards Association. 1159-2009. *IEEE Recommended Practice for Monitoring Electric Power Quality Industrial and Commercial Applications*. New York: IEEE Press; 2009.
[2] Zhang DH. Xu W. *Study on the phase sequence characteristics of interharmonics*. Proceedings of the CSEE. 2005; 25(12): 29-34.
[3] Basic D. Input current interharmonics of variable-speed drives due to motor current imbalance. *IEEE Trans on Power Delivery*. 2010; 25(4): 2797-2806.
[4] Yong J, Sun CX, Li JB, et al. Research on thyristor conduction angle characteristics in transient process of TCSC. Proceedings of the CSEE. 2008; 28(31): 88-93.
[5] Zhao W Luo An, Pan HB, et. al. *Influence of non-integer harmonics on HAPF and resolution*. Proceedings of the CSEE. 2008; 28(12): 73-78.
[6] Hsiung C. Inter-harmonic identification using group- Harmonic weighting approach based on the FFT. *IEEE Trans on Power Electronics.* 2008; 23(3): 1309- 1319.
[7] Li TY, Zhao Y, Li N, et al. *A new method for power quality detection based on HHT*. Proceedings of the CSEE. 2005; 25(17): 52-56.
[8] Vahedi H, et al. Weighting method to identify inter- harmonics based on calculating the bandwidth in group- harmonics. *Journal of Power Electronics*. 2013; 13(1): 170-176.
[9] Gong J, et al. *A new scale-frequency method for inter-harmonic detection based on continuous wavelet transform*. Computer, Mechatronics, Control and Electronic Engineering (CMCE). 2010: 137-139.
[10] Wang C, Yin XG, Wen M, et al. An Improved ipiq Reactive and Harmonic Current Detecting Method. *TELKOMNIKA Indonesian Journal of Electrical Engineering*. 2012; 10(7): 1629-1636.
[11] Wang MH, Liu HJ. *A universal definition of instantaneous power and broad-sense harmonic theory.* Proceedings of the CSEE. 2001; 21(9): 68-73.
[12] Chen DH, Xie SJ, Zhou B. *An improved synchronous reference frame method for harmonics and reactive currents detection of active power filters*. Proceedings of the CSEE. 2005; 25(20): 62-67.
[13] Sun Z, Jiang XJ, Zhu DQ. Detecting methods of reactive power, harmonic and negative -sequence current in electrified rail way systems. *Automation of Electric Power Systems*. 2003; 27(15): 53-57.
[14] Guo ZY, Zhou YQ, Guo LM. *Current detection for four-phase transmission system based on FBD method*. Proceedings of the CSEE. 2007; 27(22): 87-93.
[15] Tenti P, Mattavelli P. *A time-domain approach to power term definitions under non-sinusoidal conditions*. Sixth International Workshop on Power Definitions and Measurements under Non-Sinusoidal Conditions. Milano. 2003.
[16] Paredes HKM, Marafao FP, da Silva LCP. *A comparative analysis of FBD, PQ and CPT current decompositions-Part I: Three-phase three-wire systems*. IEEE Bucharest Power Tech Conference. Bucharest. 2009.
[17] Tenti P, Paredes HKM, Mattavelli P. Conservative power theory, a framework to approach control and accountability issues in smart microgrids. *IEEE Trans on Power Electronics*. 2011; 26(3): 664-673.
[18] Pipeleers G, Demeulenaere B, Sewers S. Robust high order repetitive control: optimal performance trade offs. *Automatica*. 2008, 44: 2628-2634.
[19] Xiao Z, Chen Y, Deng X. A Shunt Active Power Filter with Enhanced Dynamic performance using Dual-Repetitive Controller and Predictive Compensation. *International Journal of Power Electronics and Drive Systems*. 2013; 3(2): 209-217.

[20] Olm JM, Ramos GA. Costa-Castelló R. *Odd-harmonic repetitive control of an active filter under varying network frequency: a small-gain theorem-based stability analysis*. American Control Conference. Baltimore. 2010.
[21] She JH. et al. Equivalent-input-disturbance approach - analysis and application to disturbance rejection in dual-stage feed drive control system. *IEEE Trans on Mechatronics*. 2011; 16(2): 330-340.